American Meteorological Society
11th Conference on Mesoscale Processes
October 2005, Albuquerque, NM

JP4J.1 Raindrop Size Distributions and Z-R Relations in Coastal Rainfall For Periods With and Without a Radar Brightband

Brooks E. Martner[1,2], Sandra E. Yuter[3], Allen B. White[1,2], David E. Kingsmill[1,2] and F. Martin Ralph[1]

1 = NOAA Environmental Technology Laboratory, Boulder, Colorado
2 = University of Colorado Cooperative Institute for Research in Environmental Sciences
3 = Dept. of Marine, Earth and Atmospheric Sciences, North Carolina State University

1. Introduction.

The California Land-falling Jets (CALJET, 1997-98) and Pacific Land-falling Jets (PACJET, 2001-2003) experiments studied coastal winter storms in California and Oregon. One facet of the studies used new vertically pointing S-band Doppler radar profilers (S-PROF) in combination with rain gauges to observe precipitation characteristics. White et al. (2003) examined S-PROF data from the strong El Niño winter of 1997-98 for a site near Cazadero (CZD), California, about 75 km northwest of San Francisco in the mountains of the Coast Range. They discovered that the melting layer radar bright band, which is so characteristic of winter rain in most mid-latitude locations, was frequently absent above this site, even in heavy rainfall with radar echoes extending well above the freezing level. They determined that microphysical features of the rain were significantly different during these periods from times when a bright band was present. Echo tops during the non-brightband (NBB) periods were generally shallower and orographic forcing was stronger than for brightband (BB) periods.

Author contact: Brooks Martner
NOAA/ETL, 325 Broadway,
Boulder, CO 80305, USA
e-mail: brooks.martner@noaa.gov

Based on the S-PROF reflectivity and vertical velocity data, White et al (2003) concluded that the NBB rain contains more small drops and fewer large drops than the BB periods. The significantly different nature of the drop size distribution (DSD) in NBB situations, inferred from the S-PROF data, produces an empirical reflectivity-rainfall (Z-R) relation that is very different from the standard one used by NEXRAD, which seriously underestimates rain rates in these situations (White et al. 2003).

Neiman et al (2005) examined S-PROF data from three additional sites (California coast and Sierra foothills, Oregon Cascades) and three more winters and concluded that NBB rainfall is not limited to the CZD site or to El Niño winters. Depending on the particular site or year, NBB conditions contributed 18 to 50% of the total winter precipitation. Using data from the Cazadero S-PROF and from the Sacramento WSR-88D (NEXRAD) radar, Kingsmill et al (2005) studied reflectivity profiles and their relation to synoptic conditions in detail. They found that NBB situations also occur in California's flat Central Valley, although less often than in the mountains at CZD.

Each of these earlier studies inferred that the BB/NBB differences signify that markedly different precipitation formation processes are responsible for the two kinds of rainfall. Their evidence indicates that BB rain

usually results from deep, cold-top clouds that produce ice crystals, which grow by deposition, aggregation and riming to become large snowflakes which then form large raindrops when they melt. In the NBB cases, however, large snowflakes, are absent, and water drops grow by condensation aided by upslope flow and by coalescence of drops in a relatively shallow layer near the terrain.

2. HMT-04 Operations.

The earlier studies did not have the benefit of direct measurements of raindrop DSDs at the ground. The present study returned to two of the same northern California locations in the winter of 2003-2004 to further examine rain characteristics. This time, however, in addition to using S-band profilers, collocated raindrop disdrometers were employed to directly measure the DSD at the surface. A prime objective of the study is to reveal the contrasts between NBB and BB drop size distributions more definitively.

The new observations were obtained as part of NOAA's Hydrometeorology Testbed (HMT) project (http://hmt.noaa.gov). One S-band-disdrometer-rain gauge site was on the coastline at Bodega Bay (BBY) at 12 m MSL and the other was at Cazadero (CZD) approximately 10 km inland at 475 m MSL in the Coast Range, 33 km northwest of BBY. Rainfall at BBY probably experiences some orographic enhancement as maritime air masses approach the coast and abrupt topography of the adjacent mountains. Rainfall in the mountains at CZD, however, is affected by orographic enhancement to a much greater degree, as evidenced by its winter monthly rain accumulations, which typically exceed those of BBY by a factor of 2 to 3.

The S-band profilers used the extended dynamic range capability described by White et al. (2000). Using the procedure of White et al. (2003) for S-PROF data, precipitating periods were objectively categorized as brightband (BB), non-brightband (NBB), or convective (CONV). The "hybrid" category used by White *et al.* (2003) was combined with the BB category in this study, because both exhibit a definite radar brightband. Neiman *et al*. (2005) also used this consolidation of categories. Half-hour integrations of the radar data were used, which represent 52 individual vertical beams.

A Joss-Waldvogel disdrometer (JWD) counted and sized the raindrops at each profiler site. This instrument senses the momentum of drops impacting on its 50-cm^2 exposed surface (Joss and Waldvogel 1967). The disdrometer at BBY was provided to HMT by NOAA/ETL and the one at CZD was from the University of Washington. Drops were automatically counted in 20 diameter bins ranging from approximately 0.35 to 5.3 mm, and the raw data were recorded at 1-minute resolution. However, for DSD derivations, the raw data were integrated in post-processing into 10-minute samples with data quality refinements applied, as described in Section 4. Rainfall intensity (R) and equivalent radar reflectivity factor (Z) were computed from the resulting drop size spectra for every 10-minute sample, which was then tagged with the BB, NBB, or CONV classification, according to the concurrent 30-minute S-band profiler data.

3. Disdrometer and S-PROF Observations in HMT-04.

Figure 1 shows a 24-h period of S-PROF and JWD data from the BBY coastline site on 16FEB04. The storm's time-height history of reflectivity from S-PROF is displayed in the top panel, where the brightband is clearly evident between 2 and 3 km AGL part of the time. The middle panel shows rainfall intensity, accumulation, and radar reflectivity factor computed from the raw JWD data. In the lower panel, contours of the number of drops counted by the JWD are plotted as a function of time and drop size, where the smallest sizes are

near the bottom of the plot. A row of squares along the top of this panel shows the objective categorization of precipitation as brightband (blue = BB) or non-brightband (red = NBB), in this case, according to the S-PROF data for each half hour that the rain gauge recorded at least 0.5 mm of accumulation.

A number of BB-NBB transitions in the 16FEB04 storm are denoted by sequential changes of the blue and red squares in Figure 1, and associated changes are often apparent in the displayed parameters as well. Note the transition at 12:30 UTC (vertical line), for example. Although the rainfall intensity remained fairly steady, reflectivity decreased, the echo top lowered sharply (but was still generally above the freezing level), the largest drops disappeared, and there was a marked increase in the number of smaller drops, as the category changed from BB to a 2-h period of NBB rainfall.

The raw 1-minute JWD data for the entire winter season were sorted into BB, NBB, or CONV files, according to the S-PROF classification for the half-hour segments in which they occurred. Half-hour periods of little or no rain were eliminated by the classification algorithm's requirement for at least 0.5 mm of rain accumulation, according to the collocated tipping bucket rain gauge.

Table 1 shows statistics of the raw disdrometer data for the coastline (BBY) and mountain (CZD) sites. At BBY there were 63 h of BB and 65 h of NBB rain; at CZD there were 99.5 h of BB and 117 h of NBB. The NBB rain contributed approximately 36% of the total season rainfall (for categorized periods) at BBY and approximately 41% at CZD, which is within the ranges found by Neiman et al (2005) in other winters and locations. Mean rain rates for BB exceeded those for NBB by a factor of about 1.5 at both locations. Mean-volume drop diameters were almost a factor of 2 smaller and the total number of drops detected per minute was almost a factor of 2 larger for NBB compared to BB periods at both locations. Thus, non-brightband periods had more drops, but smaller ones, than brightband periods. Periods of convective rain (CONV) occurred approximately an order of magnitude less often than either of the other categories, and are not examined further in this article.

Frequency distributions of reflectivity and rainfall intensity are shown in Figure 2 for the 10-minute data. Blue lines represent BB periods and red represent NBB. Total numbers (areas under the curves) were considerably larger for CZD, where orographic lifting is strong, than for BBY. At both locations the peak of the reflectivity curves occurred at about 10-15 dBZ less for NBB than BB. The peaks of the rainfall intensity curves, however, are approximately the same for BB and NBB cases at CZD.

4. Comparison of DSDs.

For the purposes of examining DSDs and Z-R relations, the raw 1-minute JWD data were integrated into 10-minute samples, as in Hagen and Yuter (2003), to reduce statistical uncertainties and an inherent biasing of Z-R relations by increasing the number of drops in each bin (Smith et al. 1993). The instrument dead-time correction algorithm of Sheppard and Joe (1994) and other quality controls were applied to the 10-minute data. Only periods within the half-hours classified as BB or NBB were considered. By the classification criteria of White et al (2003), this meant that any half hours in which the collocated rain gauge registered less than 0.5 mm of rain accumulation ($R < 1$ mm/h) were not used, thereby eliminating half-hour periods of very light rain or dry weather. However, within each classified half hour there were often individual minutes with $R < 1$ mm/h, as measured by the JWD. Therefore, the additional criteria of $R > 0.2$ mm/h was set for using the 10-minute disdrometer data in order to minimize noisy data points.

The resulting drop size spectra are shown in Figure 3, without normalizations of the data. At both locations the NBB spectra contained larger concentrations of small drops and much smaller concentrations of large drops than the BB rainfall. The relative trends with diameter of the ratio of NBB/BB concentrations were almost identical at both locations. For example, at both sites the concentrations of the drops in the two types of rain were equal at approximately D = 1 mm; at D ~0.5 mm the ratio of NBB/BB concentrations was 3.4 and 3.6 at BBY and CZD, respectively, while at D ~3.2 mm the corresponding ratios were 0.08 and 0.09. Thus, the concentrations of large drops (D > 3 mm) were approximately an order of magnitude lower during NBB periods.

Comparisons with the well-known drop size distributions of Marshall and Palmer (M-P, 1948) are shown in Figure 4 for the CZD site. The M-P measurements were obtained in winter rain falling from stratiform clouds in southeastern Canada, and were shown to be a function of R. Here the M-P drop size equation uses the mean R value computed from the JWD data at CZD for the BB and NBB conditions, as shown in the legend of the figure. The BB spectra from CZD match the M-P spectra closely. In contrast, the NBB spectra from CZD contain much greater concentrations of small drops and much smaller concentrations of large drops than the M-P spectra.

5. Comparison of Z-R Relations.

The HMT-04 DSD data from the JWD were used to compute Z (mm^6m^{-3}) and R ($mm\ h^{-1}$) for each 10-minute categorized period, and regressions of the scatter of (Z,R) points were computed for both sites in the usual form, $Z = aR^b$. As several authors have noted recently, Z-R equations are quite sensitive to details of the regression method that is employed. In this work, R was treated as the dependent variable and the regression was computed as the least-squares fit to the $\log_{10}$-R vs. $\log_{10}$-Z data points, as recommended by Martner et al (2005). A lower cut-off threshold of R > 0.2 mm/h was used to eliminate points of very light, and possibly noise-contaminated, rain.

Figure 5 shows the JWD scatter plots and regressions for the two HMT-04 locations. The BB points are shown in black and the NBB points are in red. The correlation coefficient for the regression data exceeds 0.86 for both locations and both rainfall types. Although there is a large amount of overlap, it is clear that the NBB points occurred with generally lower reflectivity than their BB counterparts. This was especially true for the lighter rain rates at CZD. At both locations the coefficient (a) of the regression equation is considerably smaller for NBB rainfall. This agrees with the earlier findings of White et al (2003) and Kingsmill et al (2005), based on radar profiler and rain gauge data. The regressions for BB rainfall are very similar at CZD and BBY. The JWD results are summarized in Table 2.

Z-R relations were also derived from the S-PROF and rain gauge data during HMT-04. The processing was essentially the same as that used by White et al (2003). The BB and NBB time periods are the same as those used with the disdrometer data, but there are fewer points because the averaging increment is 30 minutes, instead of 10. The reflectivity data were obtained at 210 m AGL, which was considered to be the lowest useable range gate for these datasets. The regressions are linear least-squares fits to the log-R vs log-Z data, with R as the dependent variable. A lower cut-off threshold of R > 1 mm/h was used to eliminate noisy points. The resulting scatterplots and regressions are shown in Figure 6. Again, the coefficient (a) is considerably smaller for the NBB data than for BB at both locations.

However, the S-PROF reflectivities of the entire population of points from both locations in Figure 6 appear to be unreasonably small and shifted leftward by about 7 dB, compared to the corresponding JWD data in the scatter plots of Figure 5.

This suggests that the S-PROF calibration may have been seriously in error, a question that is currently unresolved. If the S-PROF points are increased by 7 dB (shifted right), then the points align closely with the JWD data and Z-R equations agree fairly well with those derived from the disdrometers.

The S-PROF/gauge Z-R relation results, adjusted by +7 dB, are summarized in Table 2, alongside the corresponding JWD results. Note the much lower coefficient (a) values for NBB rainfall in all cases on the table. This is consistent with results from all the earlier CALJET and PACJET studies, which did not have the benefit of disdrometer measurements. The small (a) value is apparently characteristic of NBB rain.

Figure 7 summarizes the disdrometer-derived Z-R equations and compares them with others commonly used in radar meteorology. All of the equations are shown in the figure's legend. The BB relations for both locations are nearly coincident and closely match the Marshall-Palmer (M-P) relation. They also agree well, except at low Z values, with the standard relation used by the NEXRAD operational radars. The NBB relations are very different, however. For NBB rain, noticeably larger rain rates are associated with most Z values, than is the case for BB, M-P, or NEXRAD.

Using the standard NEXRAD or Marshall-Palmer equations, results in significant underestimates of rain rates and accumulations, when applied to NBB situations. As indicated in Table 3, if the NEXRAD equation is applied to the entire population of Z values observed by the disdrometers in NBB situations, the estimated winter-total NBB rain accumulations would have been more than a factor of 2 too low at both locations. The M-P relation produces underestimates for NBB rain that are almost as bad. For BB rain, however, these equations underestimate accumulations by only 11-18%.

6. Summary and Conclusions.

Recent studies from CALJET and PACJET found that a large fraction of the winter rainfall in northern California and Oregon falls during periods when clouds overhead do not exhibit a melting-layer radar brightband (White et al 2003, Neiman et al 2005, Kingsmill et al 2005). They called these periods "non-brightband (NBB) rain" and deduced that microphysical characteristics of this precipitation differ in important ways from the more common brightband (BB) periods. This includes large contrasts in DSDs. Their conclusions were based on observations aloft using S-band profiling radars (S-PROF), but without the benefit of direct measurements of DSDs at the ground. The current investigation extends the earlier work by including new measurements using ground-based raindrop disdrometers.

In the winter of 2003-2004 disdrometers at two of the earlier study locations in northern California recorded 365 hours of rainfall and more than 10 million raindrops. One site (BBY) was near sea level on the coastline, and the other (CZD) was 10 km inland in the Coast Range at 475 m MSL, where orographic enhancement of rain is much stronger and more prevalent. As in the earlier studies, rainfall was objectively classified as BB, NBB, or CONV, according to data from a collocated S-PROF.

The disdrometer data confirm the microphysical inferences of the earlier work. The NBB periods contain larger concentrations of small raindrops ($D < 1$ mm) and much smaller concentrations of large drops ($D > 3$ mm) than the BB rain periods. DSDs for the BB periods are a close match to the Marshall-Palmer distribution, for the same average rain rates. The Z-R relations ($Z = a R^b$) computed from the DSDs observed by the disdrometers also revealed contrasts between BB and NBB rain that are consistent with the earlier findings based on S-PROF and rain gauge data. In agreement with the earlier work, the coefficient (a) is much smaller in all cases

for NBB than for BB periods of rain. For example, at CZD the disdrometer-derived BB relation is $Z = 169R^{1.58}$ and the NBB relation is $Z = 44R^{1.91}$. The BB relations are quite similar to the venerable Marshall-Palmer Z-R equation and (for R > 1 mm/h) agree well with the standard relation used by the WSR-88D (NEXRAD) operational radars. For NBB situations, however, these commonly employed relations significantly underestimate rain rates and accumulations.

The results have noteworthy implications for quantitative precipitation estimation by ground-based and spaceborne weather radars, especially for coastal orographic rainfall. NBB rainfall cannot be ignored, because it contributes significantly to the total winter season rainfall at some locations, and includes moderately heavy and potentially flood-producing rain at times. In the winter of 2003-2004, NBB rain at CZD contributed 41% of the season's rainfall, with intensities reaching 34 mm/h.

Acknowledgements.
HMT is an ongoing program sponsored by NOAA to improve weather and hydrologic forecasting.

9. References.

Hagen, M. and S.E. Yuter, 2003: Relations between radar reflectivity, liquid-water content, and rainfall rate during MAP SOP. *Q. J. Royal Meteor.Soc.*, **129**, 477-493.

Joss, J., and A. Waldvogel, 1967: A raindrop spectograph with automatic analysis. *Pure Appl. Geophys.*, **68**, 240-246.

Kingsmill, D.E., P.J. Neiman, F.M. Ralph, and A.B. White, 2005: Synoptic and topographic variability of northern California precipitation characteristics in landfalling winter storms observed during CALJET. *Mon. Wea. Rev.*, **133** (submitted).

Martner, B.E., V.Dubovskiy, and S.Y. Matrosov, 2005: Z-R relations from raindrop disdrometers: Effects of method dependencies and DSD data refinements. *AMS 32nd Radar Meteorology Conf.*, Albuquerque, NM, 22pp.

Neiman, P.J. G.A. Wick, F. M. Ralph, B.E. Martner, A.B. White, and D.E. Kingsmill, 2005: Wintertime nonbrightband rain in California and Oregon during CALJET and PACJET: Geographic, interannual and synoptic variability. *Mon. Wea. Rev.*, **133**, 1199-1223.

Sheppard, B.E., and P.I. Joe, 1994: Comparison of raindrop size distribution measurements by a Joss-Waldvogel disdrometer, a PMS 2DG Spectrometer, and a POSS Doppler radar. *J. Atmos. and Ocean Tech.*, **11**, 874-887.

Smith, P.L., Z. Liu, and J. Joss, 1993: A study of sampling-variability effects in raindrop size observations. *J. Appl. Meteor.*, **32**, 1259-1269.

White , A.B, J.R. Jordan, B.E. Martner, F.M. Ralph, and B.W. Bartram, 2000: Extending the dynamic range of an S-band radar for cloud and precipitation studies. *J. Atmos. and Ocean Tech.*, **19**, 1226-1234.

White, A.B., P.J. Neiman, F.M. Ralph, D.E. Kingsmill, and P.O.G. Persson, 2003: Coastal orographic rainfall proceses observed by radar during the California Land-falling Jets Experiment. *J. Hydrometeor.*, **4**, 264-282.

Table 1. Statistics for the Raw 1-Minute Disdrometer Data (Dec. 2003 - Mar. 2004).

	Bodega Bay (BBY) ETL Disdrometer			**Cazadero (CZD)** UW Disdrometer		
	BB	NBB	CONV	BB	NBB	CONV
Duration (minutes)	3780	3900	510	5970	7020	720
Rmax (mm/h)	34.3	33.0	125.3	92.3	34.2	85.1
Rmean (mm/h)	3.30	2.13	5.19	4.80	3.25	6.50
Rstdev (mm/h)	3.29	2.99	12.07	5.33	3.80	9.51
Accum. (mm/h)	207.9	138.5	44.1	477.6	380.3	78.0
Zmax (dBZ)	45.3	44.7	52.6	54.9	44.7	49.5
Dmean-vol (mm)	1.15	0.67	0.88	1.16	0.66	0.91
Mean Dmax (mm)	2.14	1.25	1.63	2.31	1.36	1.85
Drops Rate (drops/min)	393	698	416	546	1007	689

Table 2. Z-R relations ($Z = aR^b$) derived from the HMT-04 disdrometer data and from S-Band Profiler and rain gauge data. S-PROF Z values have been adjusted by +7 dB,

	Cazadero (CZD)				Bodega Bay (BBY)			
	JWD		S-PROF/Gauge		JWD		S-PROF/Gauge	
	a	b	a	b	a	b	a	b
BB	168	1.58	210	1.46	172	1.64	175	1.94
NBB	44	1.91	35	1.77	76	1.65	50	1.98

Table 3. Rainfall accumulations observed by the disdrometers and retrieved from the standard NEXRAD and Marshall-Palmer Z-R relations, using the disdrometer-observed population of Z values as input. Data include the full winter season (Dec. 2003 - Mar. 2004), using the 10-minute disdrometer samples, excluding points with R < 0.2 mm/h. Percentages of the disdrometer-observed accumulation are shown in parenthesis.

	Accumulation[1] Observed by Disdrometer	Accum. from std. NEXRAD Z-R relation	Accum. from Z-R relation of M-P
Bodega Bay (BBY):			
NBB	135.7 mm	55.8 mm (41%)	68.4 mm (50%)
BB	200.5 mm	165.8 mm (83%)	179.2 mm (89%)
Cazadero (CZD):			
NBB	372.4 mm	155.2 mm (42%)	179.6 mm (48%)
BB	473.7 mm	388.7 mm (82%)	400.2 mm (84%)

[1] = These disdrometer-observed accumulations are slightly smaller than those in Table 1, which shows the raw 1-minute data with no exclusions.

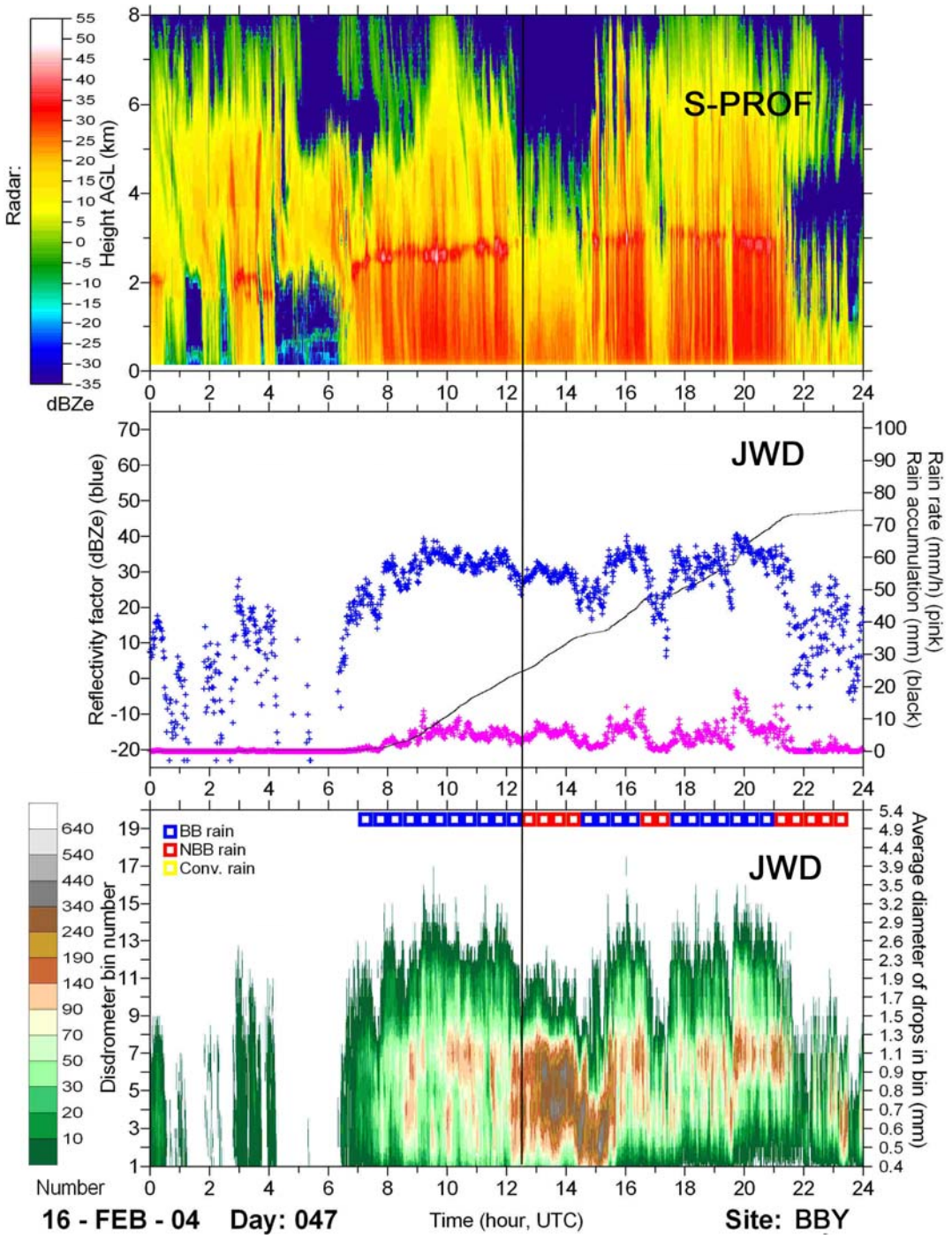

Figure 1. S-PROF and JWD data from BBY for a 24-h period on 16FEB04. Upper panel is time-height display of reflectivity. Middle panel shows rain rate, rain accumulation and radar reflectivity computed from the raw DSD data of the JWD. Bottom panel shows contoured number of drops as a function of time and diameter. Open squares indicate objective classification of half-hours as brightband (blue) or non-brightband (red) rain.

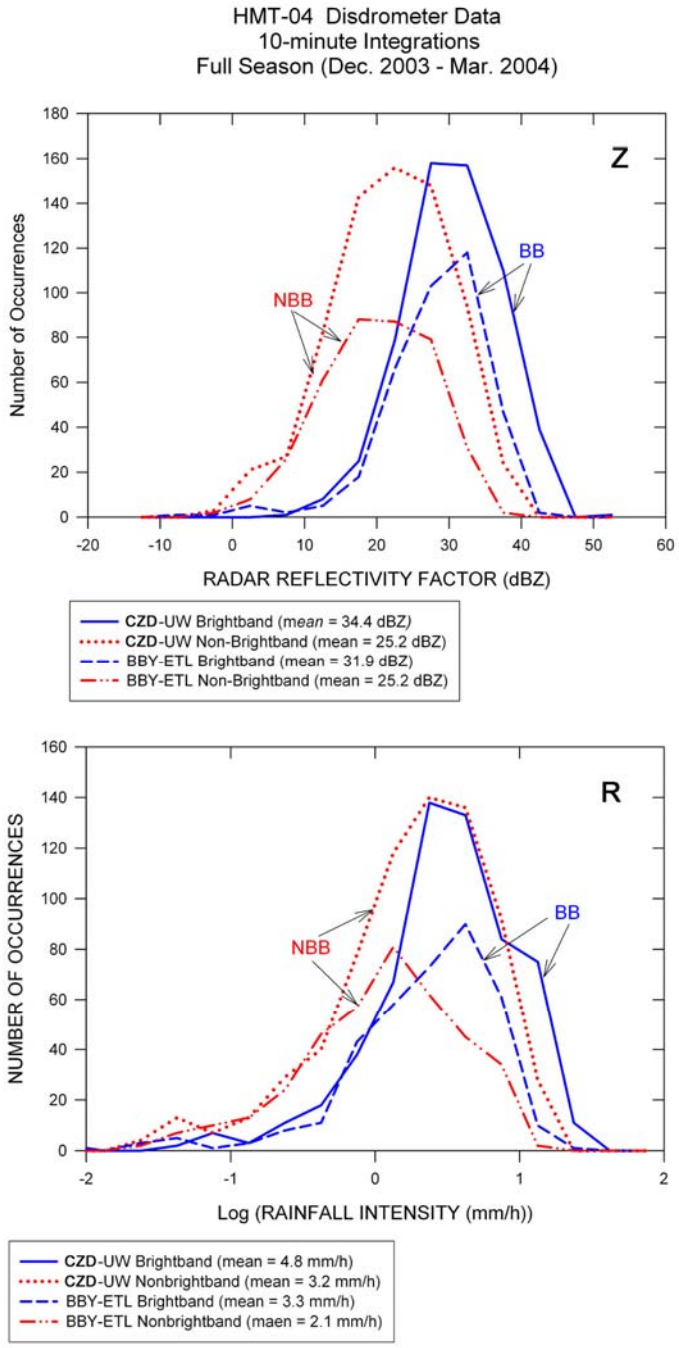

Figure 2. Frequency distributions of reflectivity (top) and rainfall intensity (bottom) from the JWD data at Cazadero (CZD) and Bodega Bay (BBY) for brightband (BB) and non-brightband (NBB) conditions.

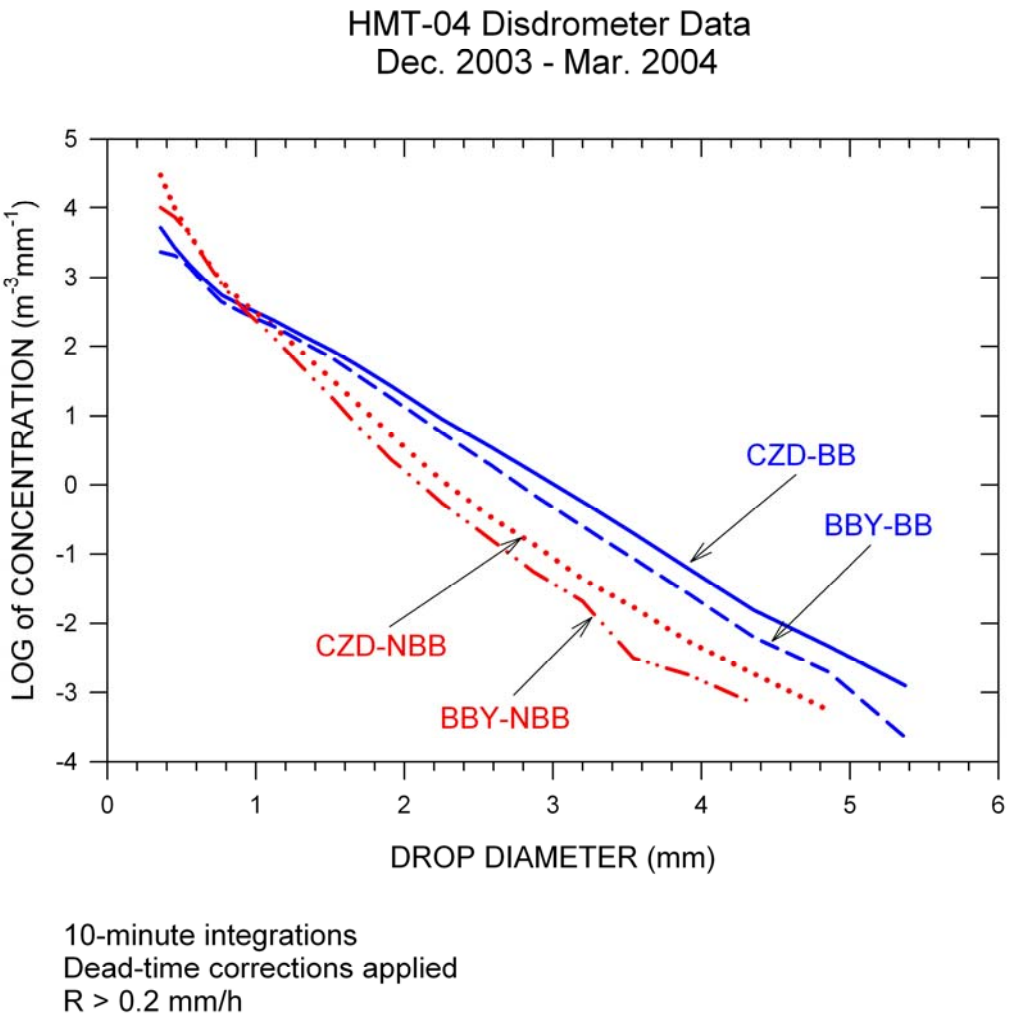

Figure 3. Drop size distributions in HMT-04 measured with raindrop disdrometers for BB (blue) and NBB (red) conditions.

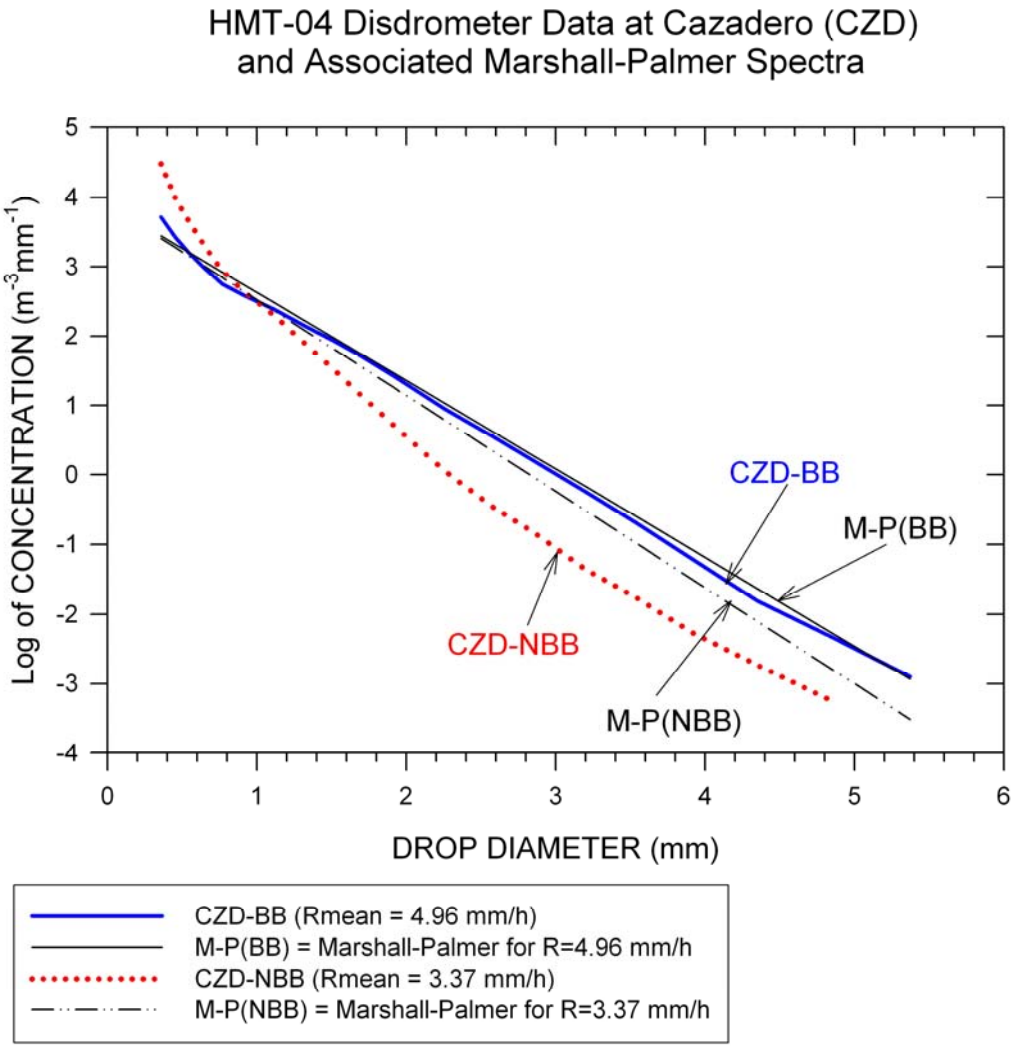

Figure 4. HMT-04 drop size distributions compared with those of Marshall and Palmer (M-P) for the same mean rainfall intensities.

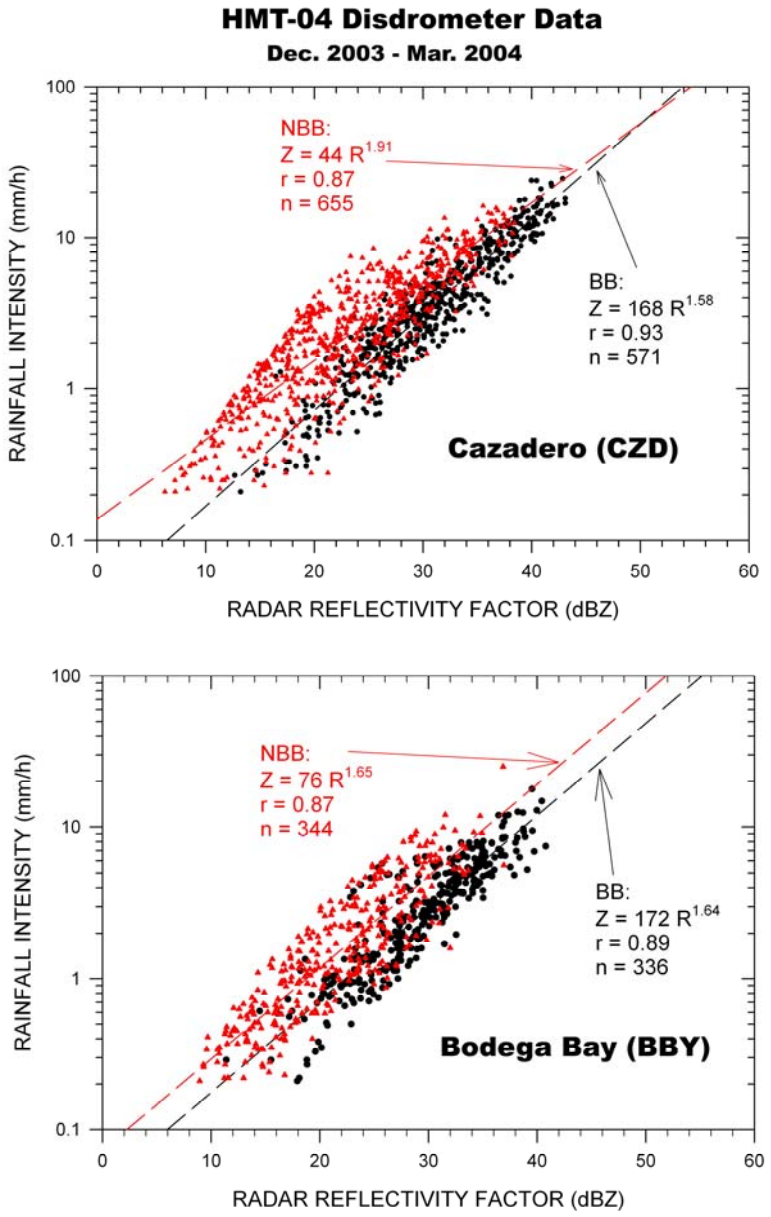

Figure 5. Z-R scatterplots and regressions from JWD data at CZD (upper panel) and BBY (lower). Each point represents 10 minutes of disdrometer data. Brightband (BB) periods are shown in black; non-brightband (NBB) in red.

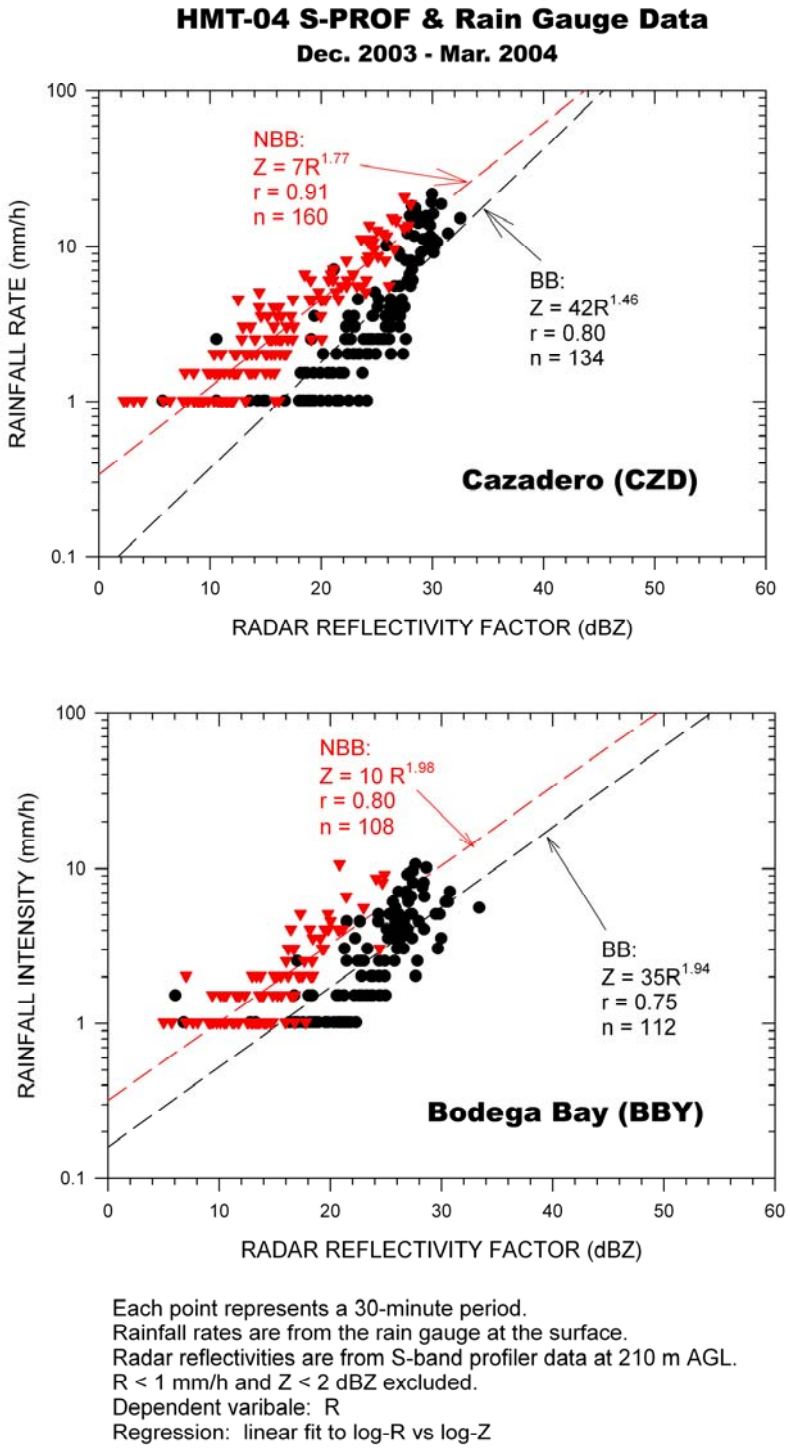

Figure 6. Z-R acatterplots and regressions for HMT-04 S-PROF and rain gauge data at CZD and BBY. Each point is a 30-minute average. BB periods are shown in black; NBB in red.

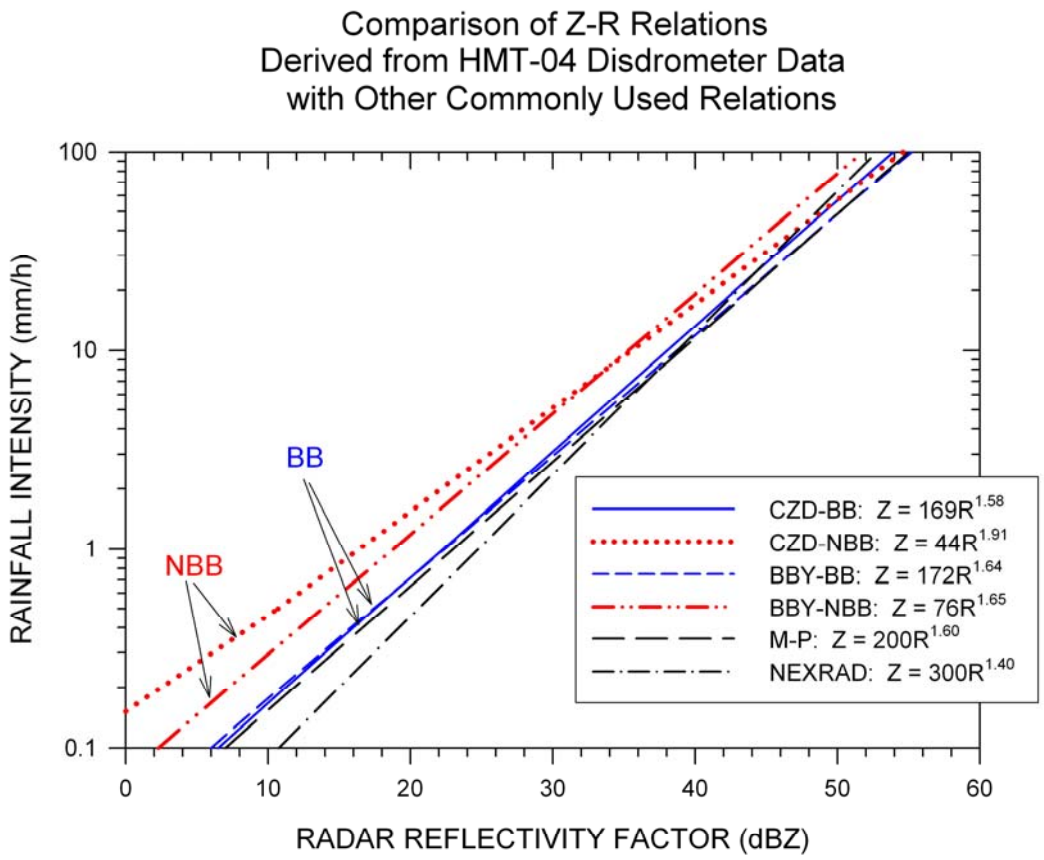

Figure 7. Comparisons of the HMT-04 disdrometer-based Z-R relations with those of Marshall and Palmer (M-P) and the standard WSR-88D (NEXRAD) equation.